Aluno Marcos Talarito Meliani

Trabalho de formatura: Comparação do programa do artigo "Validation of thermomechanical microstrutural model for closed-die forging" com o programa Form-2D.

Orientador: Prof. Dr Ronald Lesley Plaut

Validation of the thermomechanical microstructural model for closed-die forging

Maciej Pietrzyk, Zbigniew Kedzierski, Miroslaw Glowacki, Halina Kusiak and Jan Sinczak

The objective of the paper is the assessment of the predictive ability of the thermomechanical-microstructural model for the closed-die forging process. The model combines the rigid-plastic flow formulation with the finite element solution of the Fourier equation with the closed-form equations describing processes of recrystallization and grain growth. Experimental validation of the mechanical and thermal components of the model is presented in earlier publications; present work focuses on the microstructural part. Experiment includes closed-die forging of the carbon-manganese steel samples and the measurements of the grain size on the cross-sections of the forgings after the deformation. Spherical samples, which involve significant inhomogeneity of the strain and the temperature fields, have been chosen for a presentation of the results.

Gültigkeit eines thermomechanischen Modells für das Formschmieden. Gegenstand der vorliegenden Arbeit ist die Bewertung der Genauigkeit von Vorausberechnungen, die ein thermomechanisches Modell für das Formschmieden liefert. Dieses Modell verbindet die Formulierung für starr-plastisches Fließen, die FE-Lösung der Fourier-Gleichung und die Gleichungen, die Rekristallisationsprozesse und Kornwachstum beschreiben. Die Überprüfung der Rechenergebnisse anhand experimenteller Werte sowohl für die mechanischen wie die thermischen Komponenten des Modells erfolgte bereits in früheren Veröffentlichungen. Der vorliegende Teil konzentriert sich auf die Mikrostruktur. Versuche umfaßten das Formschmieden von C-Mn-Stahl. Nach erfolgter Formänderung wurde die Korngröße über dem Querschnitt der geschmiedeten Proben gemessen. Die Ergebnisse werden an kugeligen Proben, die starke Inhomogenitäten in Formänderung und Temperaturfeldern aufwiesen, erläutert.

Modern steel industry has to provide the products which satisfy the demands of the customers regarding the quality of steel, the dimensional accuracy, the grain size distribution and the mechanical properties. Thus, the mathematical models of metal forming processes should describe the thermal and mechanical events in addition to predicting the evolution of the microstructure. Advanced thermomechanical finite-element models allow the simulation of the metal flow and the heat transfer in the deformation zone with reasonable accuracy. The fact that these models supply detailed information regarding temperature fields, strain rates and strains caused an interest in the implementation of microstructural equations in the solutions and several proposals for the thermomechanical-microstructural approach have been published [1...3]. The problem of the experimental substantiation is essential here. Authors' solutions for bulk forming processes have been validated experimentally in the thermal and mechanical parts for the compression [4;5], rolling [6] and drawing [7] processes and their good predictive ability has been confirmed. Some experiments including measurements of grain size have also been performed for flat rolling [8] and rolling in grooves [9]. It seems, however, that validation of the microstructural part of the model in the non-stationary process with significantly nonuniform fields of strains and temperatures would be of a special importance. The objectives of the present paper have been formulated with the above remark in mind. The closed-die forging process has been chosen for the assessment of the predictive ability of the microstructural part of the model. Spherical forgings, which involve significant inhomogeneity of the strain and the temperature fields, have been used for the presentation of the results.

Mathematical model

Simulation of metal flow and heat transfer is based on the thermomechanical model, developed earlier for axisymmetric compression [10]. The model couples a rigid-plastic flow formulation with the finite-element solution of the general diffusion equation; transient analysis is applied to deal with the time dependence of the problem. Detailed description of the solution is given in [10;11]. The main innovations introduced in the model of the present work include the treatment of the nodes in contact with the die and those losing the contact as well as the automatic remeshing. The area-weighted average method [12] is used here for the remeshing procedure.

Modelling of the evolution of the microstructure is, in general, based on the closed form equations developed by Sellars [13] and Siwecki [14] which describe the volume fraction of the recrystallized austenite, time for 95 % recrystallization, time necessary for 50 % recrystallization, recrystallized grain size and grain growth after the deformation. The additivity rule is used to account for the temperature variations during recrystallization. The grain size directly after recrystallization is calculated using equations suggested by Sellars and Whiteman [15] (for list of symbols see **table 1**):

$$D_r = 25\left(14.925\ln\frac{10^{-9}Z}{8.5}\right)^{-\frac{1}{3}}\frac{1}{\varepsilon}D^{\frac{1}{2}} \qquad (1)$$

and by Roberts et al. [16]:

$$D_r = 6.2 + 55.7D^{0.5}\varepsilon^{-0.65}\exp\left(\frac{-35000}{RT}\right). \qquad (2)$$

Table 1. List of symbols used

D –	austenite grain size prior to deformation
D_r –	recrystallized grain size
r, z –	coordinates
R –	gas constant
T –	temperature
Z –	Zener-Hollomon parameter
ε –	true strain

Professor Dr.-Ing. Maciej Pietrzyk; Dr. hab.-Ing. Zbigniew Kedzierski; Dr.-Ing. Miroslaw Glowacki; Dipl.-Ing. Halina Kusiak; Dr.-Ing. Jan Sinczak, Department of Metal Forming, Faculty of Metallurgy and Materials Engineering, University of Mining and Metallurgy, Kraków, Poland.

Table 2. Parameters of the experiment

Stock material	heating	chemical composition
diameter 30 mm height 50 mm	temperature 1100 °C time 5 min	steel 1: 0.12%C, 0.6%Mn, 0.25%Si, 0.7%Mo, 1.0%Cr, 1.0%Ni steel 2: 0.45%C, 0.15%Si

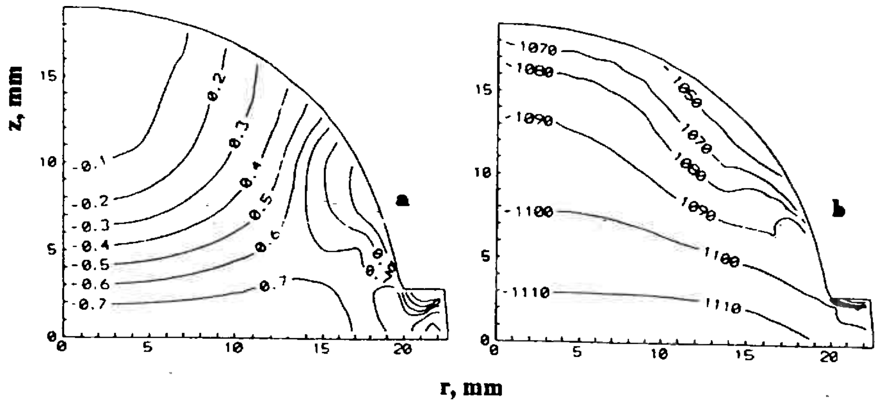

Figure 1. Distribution of the effective strain (a) and the temperature (b) on the cross-section of the spherical sample

These equations are implemented in the thermomechanical finite-element model and microstructural calculations are performed before, during and after deformation for each node of the mesh. In consequence, a distribution of the austenite grain size on the cross-section of the forging is obtained.

Experiments

Earlier substantiation of the microstructural part of the model included process of the hot compression of the axisymmetrical steel samples [11]. The objectives of the present experiment were to validate the microstructural component of the model in the industrial closed-die forging process. Forging of spherical samples has been chosen for validation. The parameters of the experiment are given in **table 2**.

After heating the cylindrical samples were withdrawn from the furnace and placed on the die within about 3 s. The forging was performed then with the initial velocity of the die of 4.5 m/s. Right after the forging the fin was cut off and the sample was quenched in water. The time interval between the end of deformation and quenching was about 7 s.

The microstructure on the cross-section of each forging has been investigated. The grain size, represented by the average diameter, has been measured in various zones on the sample's cross-section. Standard metallographic polishing techniques have been used here. Etching was done using a saturated aqueous picric acid solution with small additions of sodium dodecylbenzene sulfonate, a wetting agent. The composition of the etchant and the etching conditions were varied until the prior austenite grain structure was revealed. The grain size, represented by the average diameter, was measured in the zones at various locations on the cross-section of the forging. The measured austenite grain size before the deformation (after preheating) was 67.2 μm for steel 1 and 82.8 μm for steel 2. These values were used in all calculations.

Results and analysis

Calculated distributions of the effective strain and the temperature on the cross-section of the spherical forging are shown in **figure 1**. Due to two axes of symmetry only a quarter of the forging is considered. It can be seen in figure 1a that the maximum strains are close to the side of the forging where the fin is formed. Contrarily, a zone of very small strains appears on the vertical axis of symmetry close to the contact with the die. Analysis of the temperature field (figure 1b) shows that lowest temperatures are in the area which first had contact with the die. It is due to the intensive heat transfer to the cooler die. The heat transfer coefficient $\alpha = 13$ kW/m^{2}K was used in all calculations. The highest temperatures in figure 1b are observed in the centre of the sample, where the effect of some deformation heating can be well seen. The time-temperature profiles for four locations on the cross-section of the forging are presented in **figure 2**. The air cooling after exit from the furnace can be seen first, then some deformation heating followed by air cooling after deformation and finally quenching in water. Different cooling rates for various locations can be well seen in the figure.

The micrographs taken at the various locations on the cross-section of both samples are shown in **figures 3 and 4**. Differences between grain sizes at various parts of the forgings can be seen with the naked eye, in particular for the steel 1. Since the steel 2 presented some difficulties in etching, the photographs for this steel are of poorer quality. The coarser grains for both steels can be observed in the area of the smallest strains in figure 1a, located on the vertical axis of symmetry close to the contact surface.

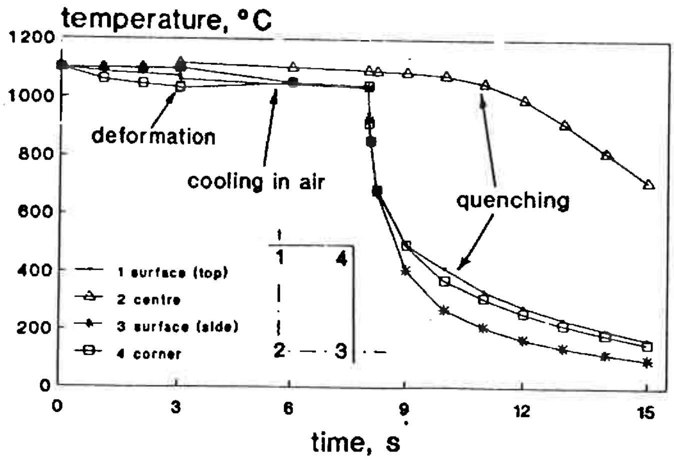

Figure 2. Time temperature profiles during the process of forging of the spherical sample

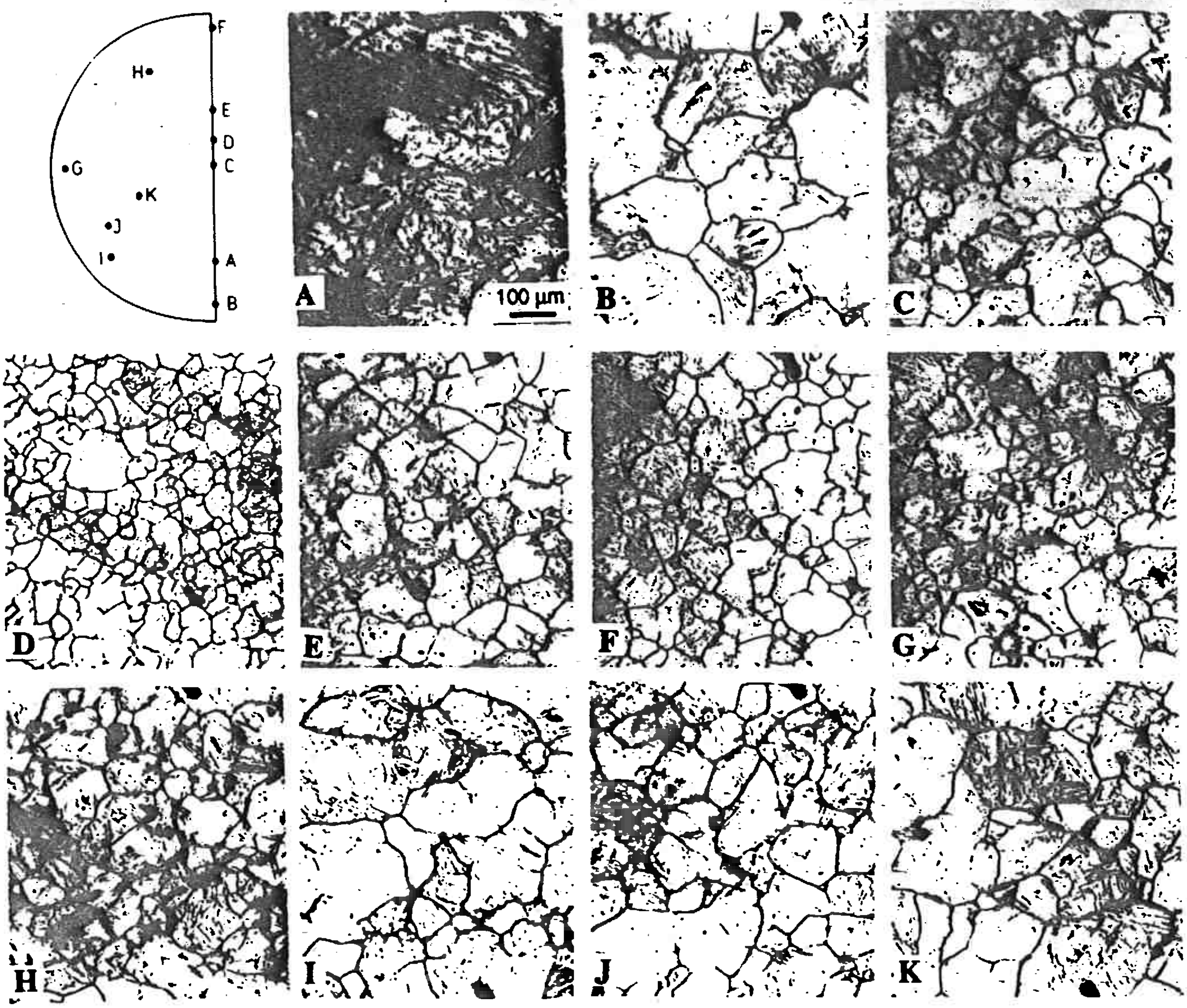

Figure 3. Micrographs taken in various locations on the cross-section of the spherical forging for steel 1

The finest grains can be observed in the area of the largest strains in figure 1a located close to the fin. Quantitative results of the measurements of the grain size are compared with the calculations in **figures 5 and 6**. Theoretical curves are presented for equations (1) and (2). Experimental data are marked by the bold face numbers in figures 5a and 6a. Analysis of the results presented in figures 5 and 6 shows very good qualitative agreement between the measured and calculated distributions of the grain size. Character of the distribution is similar for the experiment and calculations based on both equations by Sellars and Whiteman [15] and by Roberts et al. [16]. Quantitative analysis shows some discrepancies, which are larger for equation (4) by Roberts et al. [16]. In both considered cases the measurements show a lack of symmetry with respect to the horizontal axis, while this symmetry was assumed in the theoretical model. The lack of symmetry in the measurements is due to the fact that under real forging conditions the sample's contact with the lower die is slightly longer than that with the upper die and, in consequence, the temperatures in the lower part of the sphere are slightly lower. Because of the lack of the precise data regarding the times of contact this fact is not accounted for in the calculations.

Analysis of the results presented in figures 5 and 6 shows that the calculated difference in the austenite grain size between two steels is negligible. Indeed, differences in the initial grain sizes (67.2 μm for steel 1 and 82.8 μm for steel 2) resulted in a few microns difference of the grain size at the beginning of quenching. Measurements show much larger differences, reaching 50 % in some areas (figures 5a and 6a). It seems that the prediction of the grain growth is responsible for these discrepancies. Calculated distributions of the recrystallized grain size presented in **figure 7** show significant differences between the two steels, the grains being noticeably coarser for steel 2. Grain growth during 5 s of air cooling, simulated using the equation by Roberts et al. [16], decreases differences between the steels leading to grains only a few microns larger for the steel 2 in figures 5 and 6. Analysis of the results of the calculations shows that in the areas of the largest grains the recrystallization time was close to 5 s and there was no influence of the grain growth observed. Contrarily, the recrystallization time in the areas of the small grains was very short and the influence of the grain growth was essential there, the growth being faster for steel 1. It may be suggested that the equation describing grain growth in the typical carbon-manganese steels (Roberts et al. [16]) introduces an error to calculations for steel 1 which contains some alloying.

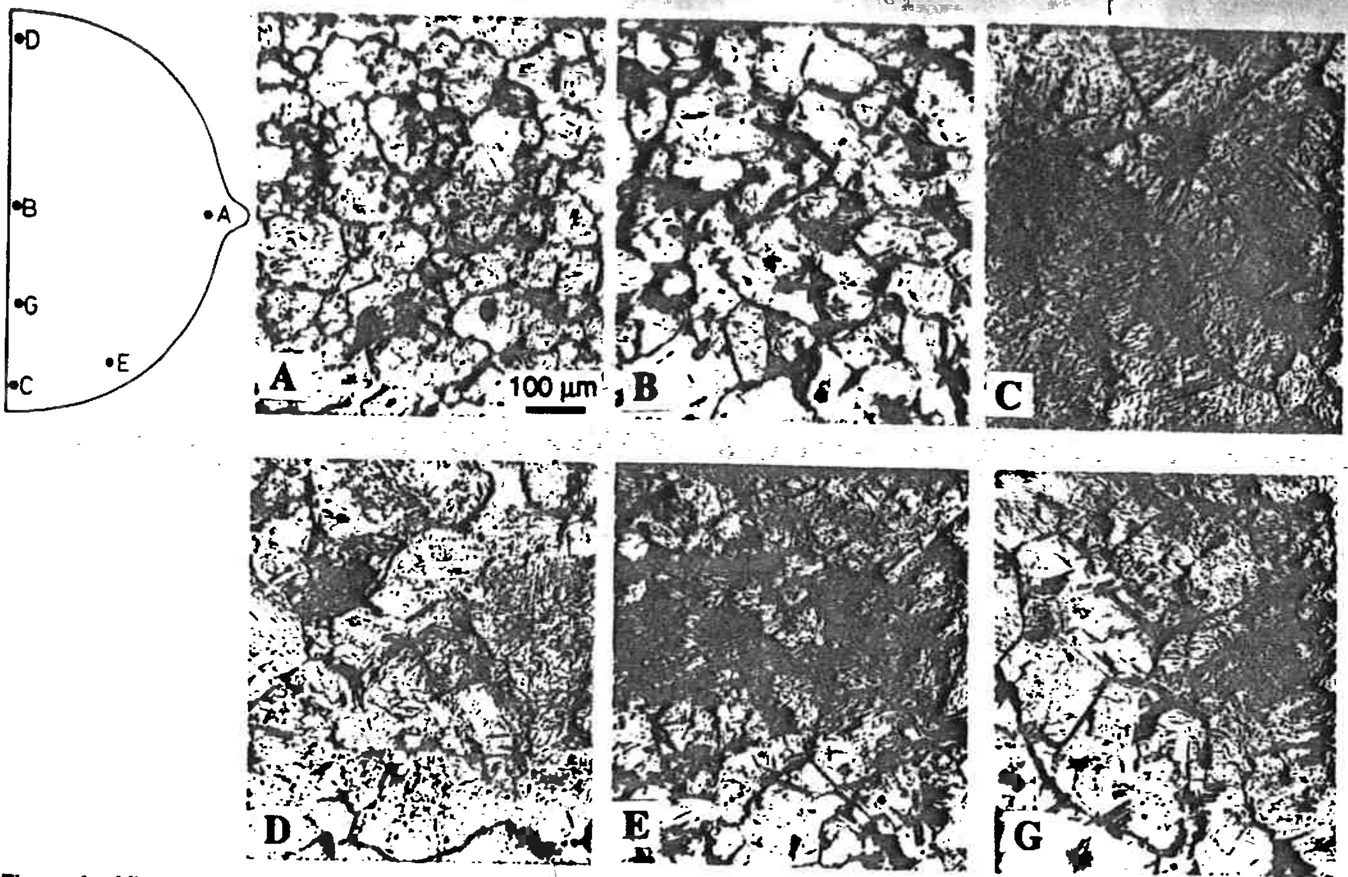

Figure 4. Micrographs taken in various locations on the cross-section of the spherical forging for steel 2

In order to present its abilities, the model is used here to calculate distributions of the effective strain, temperature and grain size in various closed-die forging processes. Typical results for forging with two axes of symmetry are presented in figures 8 and 9. The stock material was a cylindrical sample with a radius of 96 mm and a height of 52 mm. The sample was assumed to be heated to a uniform temperature of 1100 °C, withdrawn from the furnace and cooled in air for a few seconds before forging. In consequence, the forging process began with the nonuniform temperature on the cross-section of the sample which resulted from the air cooling. Figure 8 shows the distributions of the effective strain (upper part) and the temperature (lower part) just afer deformation. Significant nonuniformity of strains can be seen in this figure. The largest strains appear in the central part of the forging and, of course, in the fin. The largest strain in the fin was 2.6, but due to the limitations of the graphic program it is not shown in figure 8a. The lowest strains, below 0.6, are in the centres of thicker parts of the cross-section. The temperature field, as expected, shows very steep gradients in the areas close to the contact surface. In spite of the heated die (400 °C), significant heat transfer to the tool is still observed. Some deformation heating of the central part of the forging can also be seen in figure 8b. Notice that the stock sample was heated to a uniform temperature of 1100 °C in the furnace and then cooled in air for few seconds. Distribution of the austenite grain size after recrystallization is shown in figure 9. The results in this figure indicate that the grain sizes reflect the fields of strains and temperatures presented earlier.

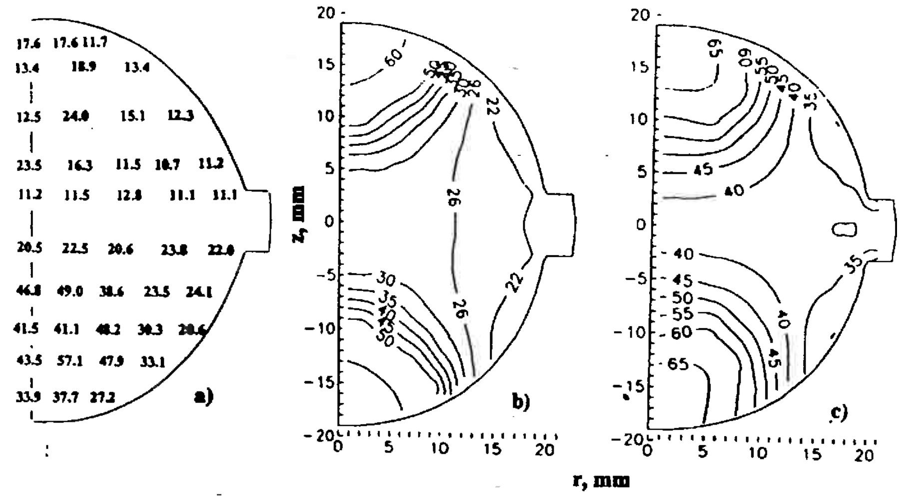

Figure 5. Austenite grain size on the cross-section of the spherical forging obtained from the measurements (a) and calculations using equation by Sellars and Whiteman [15] (b) and by Roberts et al. [16] (c) for steel 1

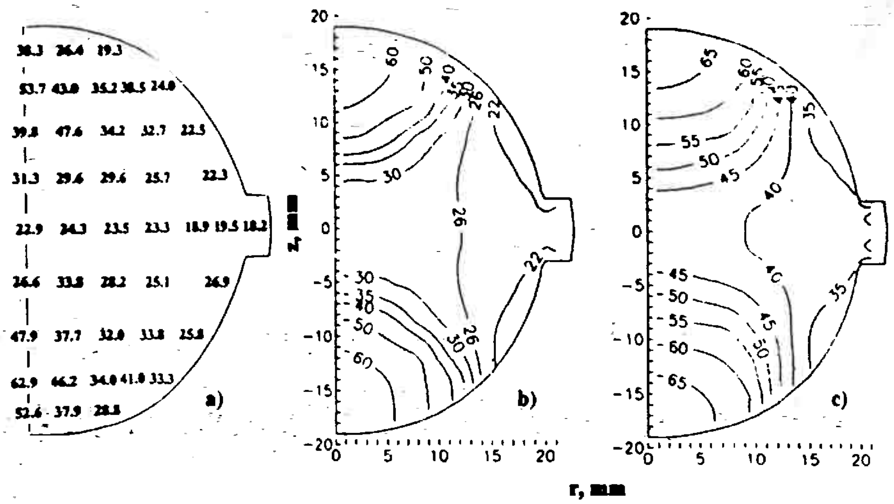

Figure 6. Austenite grain size on the cross-section of the spherical forging obtained from the measurements (a) and calculations using equation by Sellars and Whiteman [15] (b) and by Roberts et al. [16] (c) for steel 2

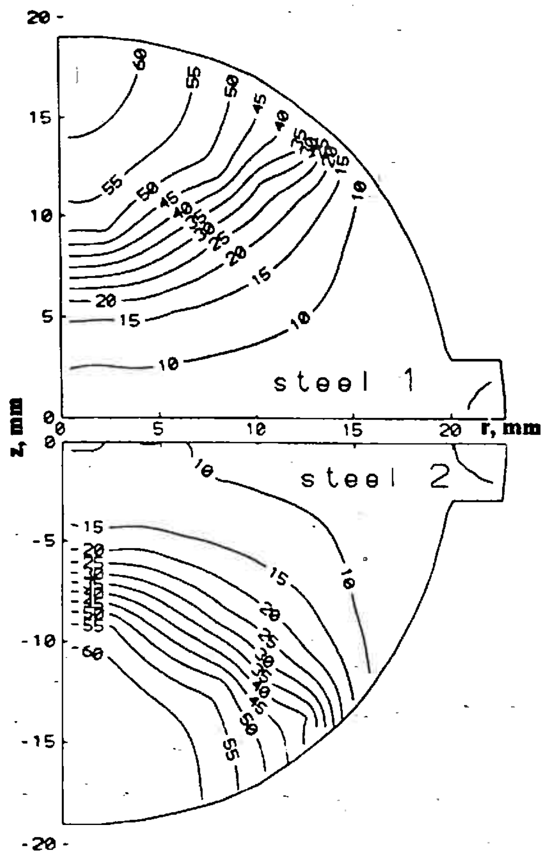

Figure 7. Calculated distributions of the recrystallized austenite grain size on the cross-section of the spherical forging for both steels

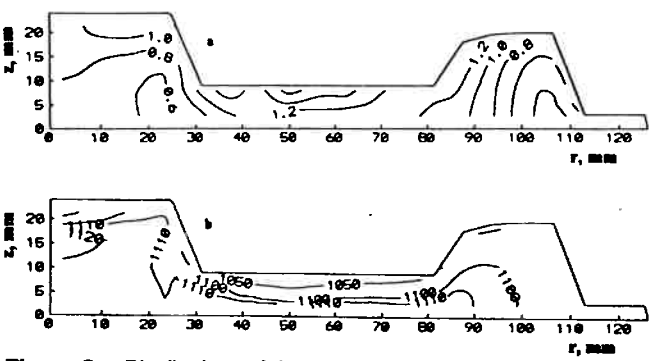

Figure 8. Distributions of the effective strain (a) and the temperature (b) on the cross-section of the axisymmetrical forging

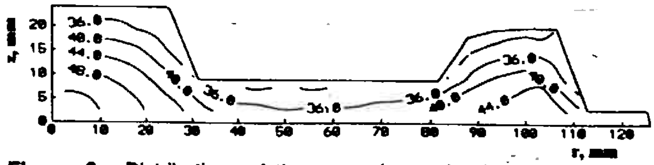

Figure 9. Distributions of the austenite grain size on the cross-section of the axisymmetrical forging

The finest grains appear in the regions of largest strains and lowest temperatures.

Conclusions

The thermomechanical microstructural model has been validated experimentally and successfully used to simulate the closed-die forging process. Experimental substantiation of the model includes metal flow, heat transfer and microstructure evolution. Substantiation of the model, performed for the forging of the spherical samples, confirmed its good predictive ability. Very good qualitative agreement between the measurements and the calculations of the austenite grain size has been obtained for both Sellars and Whiteman and for Roberts et al. equations. Quantitative comparison shows some discrepancies which are smaller for the Sellars and Whiteman equation. It seems that difficulties with the precise assessment of the forging conditions were the main reason of these discrepancies. The real time of the contact of the workpiece with the die is particularly difficult to evaluate. Moreover, the closed form equations describing processes of recrystallization and grain growth do not take an advantage from the detailed and precise information regarding the time-dependent temperature and strain fields which is supplied by the thermomechanical finite-element model. It seems that an application of a more elaborate microstructural model based on the analysis of the probability distribution of the dislocation density would improve the quantitative assessment of the problem.

Acknowledgements

Financial support of The Polish Committee for Scientific Research (grant 7.0520 91 01) is gratefully acknowledged.

(A 00 894; received: 10. September 1993;
in revised form: 5. December 1993)

References

[1] *Beynon, J. H.; Brown, P. R.; Mizban, S. I.; Ponter, A. R. S.; Sellars, C. M.*: Proc. Numiform'86, [eds.:] K. Mattiasson, A. Samuelsson, R. D. Wood, O. C. Zienkiewicz, Gothenburg, 1986, p. 213/18.
[2] *Zouhar, G.; Hofgen, H.*: Proc. 8th PTD Conf., Dearborn, 1988, p. 23/40.
[3] *Pietrzyk, M.*: Proc. 11th Conf. Computer Methods in Mechanics, [eds.:] W. Gilewski, L. Chodor, Kielce, 1993, p. 715/22.
[4] *Glowacki, M.; Pietrzyk, M.*: J. Mech. Work. Techn. 19 (1989), p. 295/303.
[5] *Pietrzyk, M.; Lenard, J. G.*: Proc. Conf. CMEM V [eds.:] A. Sousa, C. A. Brebbia and G. M. Carlomagno, Montreal, 1991, p. 449/56.
[6] *Pietrzyk, M.; Lenard, J. G.*: Thermal Mechanical Modelling of the Flat Rolling Process, Springer Verlag, Berlin, 1991.
[7] *Sadok, L.; Packo, M.; Pietrzyk, M.; Malinowski, Z.*: Proc. Conf. CMEM V, [eds.:] A. Sousa, C. A. Brebbia and G. M. Carlomagno, Montreal, 1991, p. 481/92.
[8] *Pietrzyk, M.; Kedzierski, Z.; Kusiak, H.; Madej, W.; Lenard, J. G.*: steel res. 64 (1993), p. 549/56.
[9] *Glowacki, M.; Kedzierski, Z.; Kusiak, H.; Madej, W.; Pietrzyk, M.*: J. Mat. Proc. Techn. 34 (1992), p. 509/16.
[10] *Pietrzyk, M.*: Hutnik 58 (1991), p. 60/63.
[11] *Pietrzyk, M.; Glowacki, M.; Lenard, J. G.*: J. Mat. Proc. Techn. 1993, to be published.
[12] *Kobayashi, S.; Oh, S.-I.; Altan, T.*: Metal Forming and the Finite Element Method, Oxford University Press, New York – Oxford, 1989.
[13] *Siwecki, T.*: Proc. Symp. Microalloyed Vanadium Steels, [eds.:] M. Korchynsky, S. Gorczyca and M. Blicharski, Krakow, 1990, p. 63/78.
[14] *Sellars, C. M.*: Mat. Sci. Techn. 6 (1990), p. 1072/81.
[15] *Sellars, C. M.; Whiteman, A. J.*: Met. Sci. 13 (1979), p. 187/94.
[16] *Roberts, W.; Sandberg, A.; Siwecki, T.; Werlefors, T.*: Proc. Conf. HSLA Steels, Techn. & Applications, ASM, Philadelphia, 1983, p. 67/84.

INTRODUÇÃO

O presente trabalho tem por objetivo comparar os resultados do artigo " Validation of the thermomechanical microstrutural model for closed-die forging".

O objetivo do artigo acima é verificar a habilidade de predizer do modelo termomecanico-microestrutural no processo de forjamento em matriz fechada.

O modelo combina a formulação do fluxo plástico-rigido com a solução dos elementos finitos da equação de Fourier e com as equações descrevendo processos de recristalização e crescimento de grão.

Compara-se os resultados obtidos pelos autores do artigo com os resultados obtidos na simulação do forjamento usando o programa de elementos finitos Form-2d,Quantor Ltd., Versão 2.12 ,32-bit Moscou ,1996.

O programa Form-2d forneceu a distribuição da temperatura,deformação e taxa de deformação no forjado.O tamanho de grão recristalizado não foi calculado por este programa .

INTRODUÇÃO TEORICA

O objetivo da moderna indústria do aço é fornecer produtos que tenham precisão dimensional, distribuição de tamanho de grão e propriedades mecânicas adequadas.Modelos avançados de elementos finitos termomecânicos permitem a simulação do fluxo metálico e a transferencia de calor na zona de deformação com razoavel precisão.O fato que esses modelos suprem informações detalhadas a respeito do campo de temperatura, taxa de deformação, e deformação causam um interesse na implementação de equações microestruturais . Soluções e varias propostas para abordagem da relação termomecânica-microestrura foram publicadas. Predições de modelos em processos de compressão, laminação, e trefilação foram confirmadas experimentalmente e suas habilidades de previsão foram comfirmadas.

Entretanto a comprovação da parte microestrural do modelo em processo em processo não-estacionário com significatvos campos não uniformes de deformação e temperatura tem uma importância especial e é analisada neste trabalho.

MODELO MATEMÁTICO

Simulação de fluxo metálico e transferência de calor é baseada no modelo termomecânico , desenvolvido inicialmente para compressão axisimétrica .O modelo combina formulação da fluxo plástico-rígido com a solução de elementos finitos da equação de difusão geral ;análise do transiente é aplicada para tratar com a dependência do tempo do problema. No artigo analisado é feito um tratamento dos nós em contato com a matriz e aqueles que perdem contato com ela e refaz-se a malha automáticamente . O método da média do peso da área é usado aqui para o procedimento de refazer a malha.

O modelamento da evolução da microestrurura é, em geral, baseado nas equações desenvolvidas por Sellars e Siwecki que descrevem a fração volumétrica da austenita, com tempo de recristalização para 95% de recristalização ,tempo necessário para 50% de recristalização , tamanho de grão depois da deformação . A regra da aditividade é usada para contabilizar as variações de temperatura durante a recristalização. O tamanho de grão depois da recristalização é calculado usando as equações sugeridas Sellars e Whitman e por Roberts e outros que são dadas a seguir

equação de Sellars e Whiteman

$$DR=25(14,925\ln((10^{-9})Z/8,5))^{-2/3}D^{-1}D_I^{1/2}$$

$Z=(TD)\exp(Q/(RT))$ $\quad\quad$ $R=8,31[J.mol^{-1}.K^{-1}]$

$Q=312[KJ.mol^{-1}]$

Equação de Roberts

$$DR=6,2+55,7D_I^{0,5}D^{-0,65}\exp(35000/(RT))$$

Lista de simbolos

D_I=tamanho de grão antes da deformação

D_R=tamanho de grão recristalizado

R=constante dos gases

T=temperatura

Z=parametro de Zener-Hollomon

D=deformação verdadeira

TD=taxa de deformação

Estas equações são implementadas no modelo de elementos finitos termomecânicos e calculos microestruturais são antes , durante, e depois da deformação para cada nó da malha. em consequência , uma distribuição do tamanho de grão austenítico na secção transversal do forjado é obtida.

PROCEDIMENTO

No artigo considerado o tarugo era de aço 1045, foi aquecido a uma temperatura uniforme de 1100 ^{o}C ,sofreu resfriamento ao ar por poucos segundos . O forjamento foi feito em um martelo de velocidade inicial de 4,5 m/s. O coeficiente de transferência de calor foi 13 W/m^2K. O tamanho de grão inicial foi 82,8 um.

A simulação efetuada no programa Form-2D foi realizada em aço 1020, num martelo de contra-golpe de velocidade inicial relativa das ferramentas de 5.212 mm/s.O coeficiente de transferencia de calor assumiu vários valores com o objetivo de obter uma distribuição de temperatura no forjado semelhante à obtida pela simulação do artigo considerado.

A temperatura inicial foi 1100 ^{0}C e suposto um resfriamento ao ar após sair do forno antes do forjamento de 5 s.O resfriamento do forjado na ferramenta antes da deformação foi considerado 5 s também.

ANÁLISE DOS RESULTADOS

A forma de apresentar os resultados quanto a temperatura, deformação e taxa de deformação é diferente no artigo e no programa Form-2D.

No artigo a forma de apresentação é através de linhas que possuem um mesmo valor ,já no programa Form-2D os resultados são apresentados numa faixa de valores.

Para se obter resultados semelhantes o coeficiente de transferencia de calor assumiu vários valores na faixa de 13 a 20 W/m^2K .Para a comparação foi considerado o valor 16 W/m^2K ,no qual se obteve um resultado mais próximo ao artigo.

No artigo, devido à simetria do forjado ,foi analisada uma parte correspondente a 1/4 do forjado. Esta parte foi dividida em 3 regiões comforme a fig. 1.

Na região 1 no artigo a temperatura assumi 2 valores :1110 ^0C e 1120 ^0C (fig. 2).

No programa Form-2D a faixa de temperaturas é 1086 a 1105 ^0C na região central e na faixa de 1067 a 1086 ^0C nas extremidades (fig. 3).

Portanto, pelo programa Form-2D, esta região é mais fria que no artigo o que é razoável pois esta região ficou mais tempo em contato com a matriz e deformou-se relativamente pouco.

Na fronteira entre as regiões 1 e 2,pelo programa Form-2D,ocorre as mais altas temperaturas entre as faixas de 1125 a 1144 ^0C e 1144 a 1167 ^0C, portanto uma temperatura muito superior ao programa do artigo que é 1100 ^0C.No programa Form-2D a maior parte desta região central esta na faixa 1105 a 1125 ^0C.

Quanto a região 2 as temperaturas , pelo programa do artigo, são 1050,1100,1110 ^0C enquanto que no programa Form-2D há 2 faixas ,uma à esquerda entre 1086 a 1105 ^0C e outra à direita entre 1067 a 1086 ^0C. Portanto há uma certa discrepância entre as distribuições de temperatura dos 2 programas ,mas ambos os programas mostram que houve resfriamento na superfície devido ao contato com a matriz.

Pelo programa Form-2D há uma liberação de calor devido à deformação que aumenta a temperatura na região entre as regiões 1 e 2 de uma quantidade maior que a variação de temperatura do programa do artigo.

Na região 3 pelo artigo só é dada a temperaturade 1100 ^0C.

Pelo programa Form-2D tem-se no canto superior à direita a temperatura mais baixa na faixa 1025 a 1048 ^0C;a maior parte ,contudo, fica na faixa de 1086 a 1105 ^0C, portanto coerente com o artigo.

No artigo não há a temperatura da rebarba, mas no programa Form-2D a temperatura chega a 1144 a 1167 ^0C na parte superior central. A maior parte da rebarba está a uma temperatura na faixa de 1125 a 1144 ^0C.

Portanto há uma certa discrepância entre as distribuições de temperatura nos 2 programas.

A deformação real também é dada em linhas de mesmo valor no artigo (fig.4) e em faixas de valores no programa Form-2D (fig.5).

Na região 1 o artigo fornece 3 valores :1,0; 0,8 ; 0,6.

O programa Form-2D fornece basicmente 2 faixas d valores.A esquerda uma faixa que assume os valores $5{,}774.10^{-13}$ a 0,6521 e uma faixa à direita assumindo os valores 0,6521 a 1,203.

O valor 1,0 do artigo excede o maior valor da faixa que é 0,6521 e o valor de deformação 0,6 fornecido pelo artigo assumi valor menor que o limite inferior da faixa do programa Form-2d que é 0,6521.

Além do mais no artigo as deformações diminuem de valor no sentido da região entre as regiões 1 e 2 que possue as maiores defomações pelo programa Form-2D que chega a uma faixa de 3,405 a 4,057 de deformação.

A região entre as regiões 1 e 2 tem as maiores deformações pelo programa Form-2D, coerente com as altas temperaturas obtidas nesta região.

As regiões 2 e 3 são basicamente ocupadas por uma faixa , no programa Form-2D, que assumi os valores de 0,6521 a 1,203.

No artigo é dado só o valor 1,2 de deformação na região 2 que é o limite superior da faixa do programa Form-2D.

Na região 3 são dados 3 valores no artigo: 1,2 ;1,0 e 0,8 de deformação. Esses valores diminuem no sentido em que as deformações são maiores que é a região da rebarba, que no programa Form-2D chega a faixa de deformação 3,405 a 4,057, enquanto que no artigo é citado

2,6 como deformação na rebarba que não é mostrado na figura devido as limitações do programa usado.

A taxa de deformação não é dada no artigo mas é estimada em 3 regiões .Para isso foi usada a equação de Sellars e Whiteman. obteve-se a tabela abaixo.

	D_R	$t(^0C)$	deformação	T.D.(s^{-1})
ponto 1	40,0	1110	0,8	0,0491
ponto 2	36,0	1100	1,2	0,0254
ponto 3	40,0	1100	0,8	0,0400

O valor médio da taxa de deformação é 0,0387 s^{-1} .

No programa Form-2D obtem-se para a quase totalidade do forjado uma faixa que assumi os valores comprendidos entre 0,1297 a 348,9 s^{-1} (fig. 6),portanto uma faixa muito ampla de valores,sendo que o valor inferior da faixa é superior ao valor médio obtido para a taxa de deformação do artigo.

Há uma pequena região entre as regiões 2 e 3 que assumi uma faixa de valores para a taxa de deformação de 348,9 a643,4 s^{-1} .

O ponto 2 da tabela possui valores desta região e a taxa de deformação obtida é 0,0254 s^{-1} .

Portanto há uma discrepância muito grande entre a taxa de deformação calculada pelo artigo e aquela obtida pelo prgrama Form-2D.

Valores calculados para o tamanho de grão pela equação de Sellars-Whiteman usando a taxa de deformação média dada pelo programa Form-2D que é 175 s^{-1} fornecem valores inferiores a 10 um. A equação de Roberts ,usando os valores fornecidos pelo artigo ,fornece também uma distribuição de tamanho de grão um pouco inferior à fornecida pelo artigo.

CONCLUSÃO

Os valores obtidos no artigo e no programa Form-2D para temperatura e deformação são próximos, as diferenças podendo ser devidas a maneira diferente dos 2 programas apresentarem seus resultados, já a taxa de deformação apresenta uma discrepância maior entre os resultados obtidos nos 2 programas.

Para efeito de comparação entre a distribuição de tamanho de grão do artigo (fig. 10) é fornecido na fig.7 uma distribuição de tamanho de grão calculado usando a equação de Roberts e os valores médios das faixas obtidas no programa Form-2D.

As fig. 8 e fig.9 fornecem os valores médios da deformação e da temperatura obtidos no programa Form-2D.

Os tamanhos de grão obtidos são ligeiramente inferiores ao do artigo.

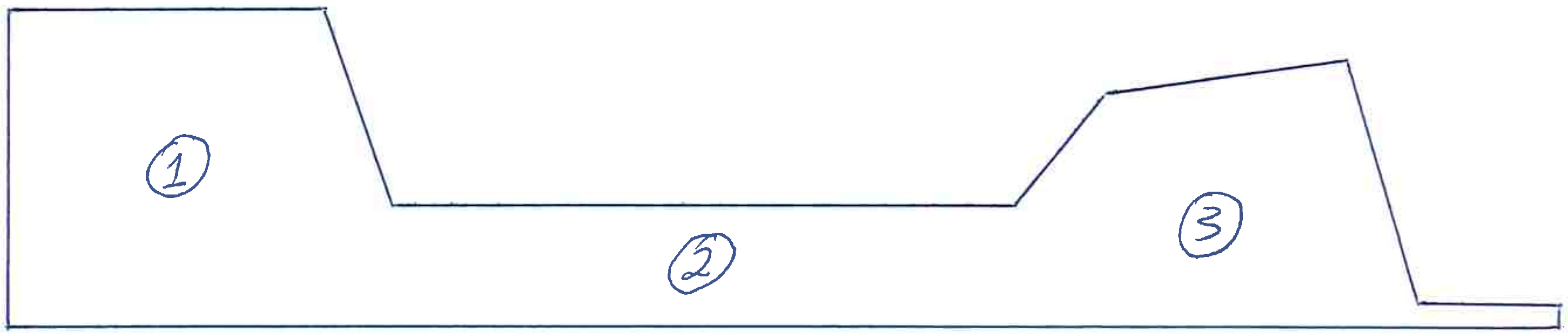

FIG. 1

grain size on the cross-section of the spherical forging for both steels

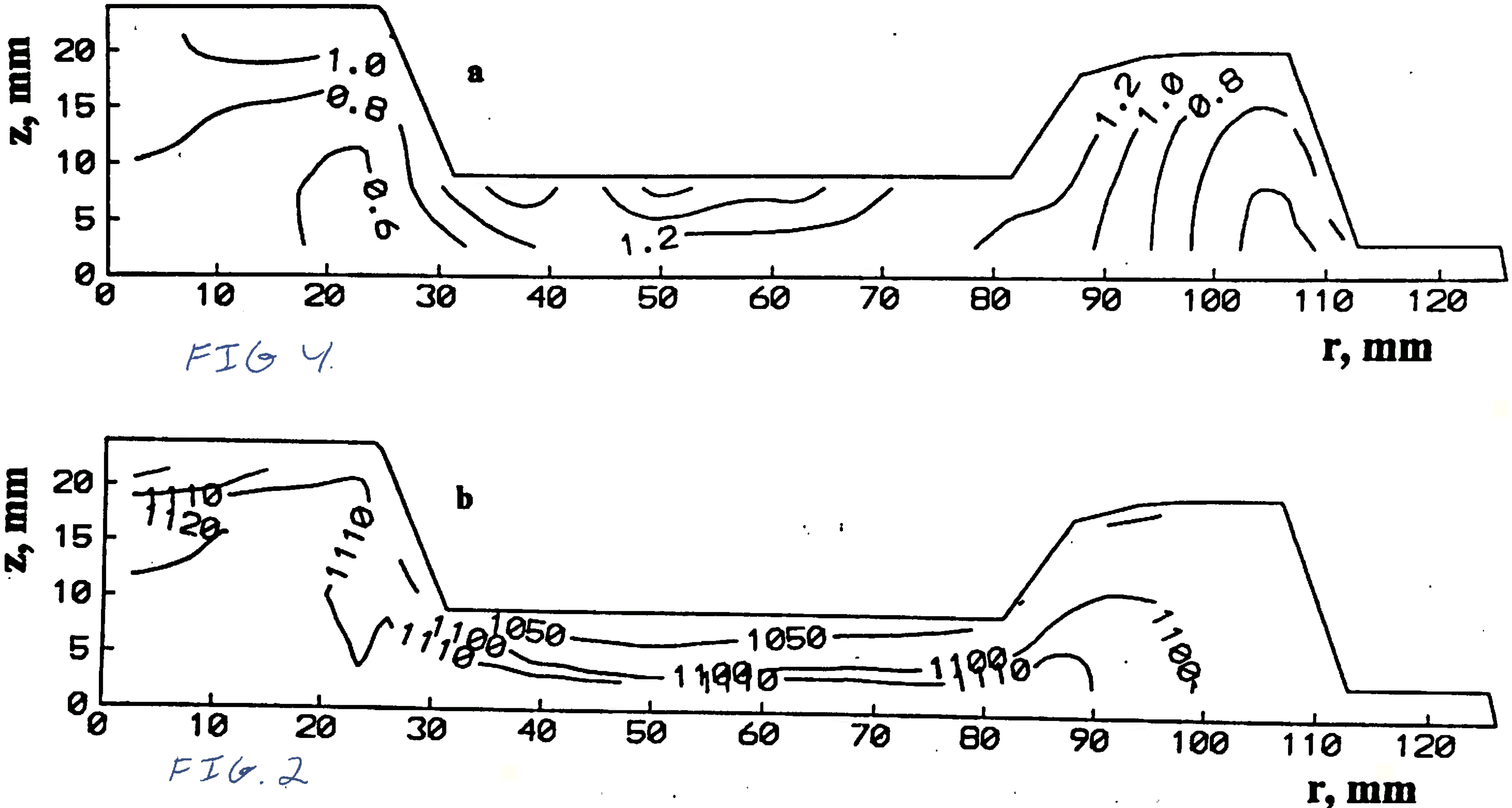

Figure 8. Distributions of the effective strain (a) and the temperature (b) on the cross-section of the axisymmetrical forging

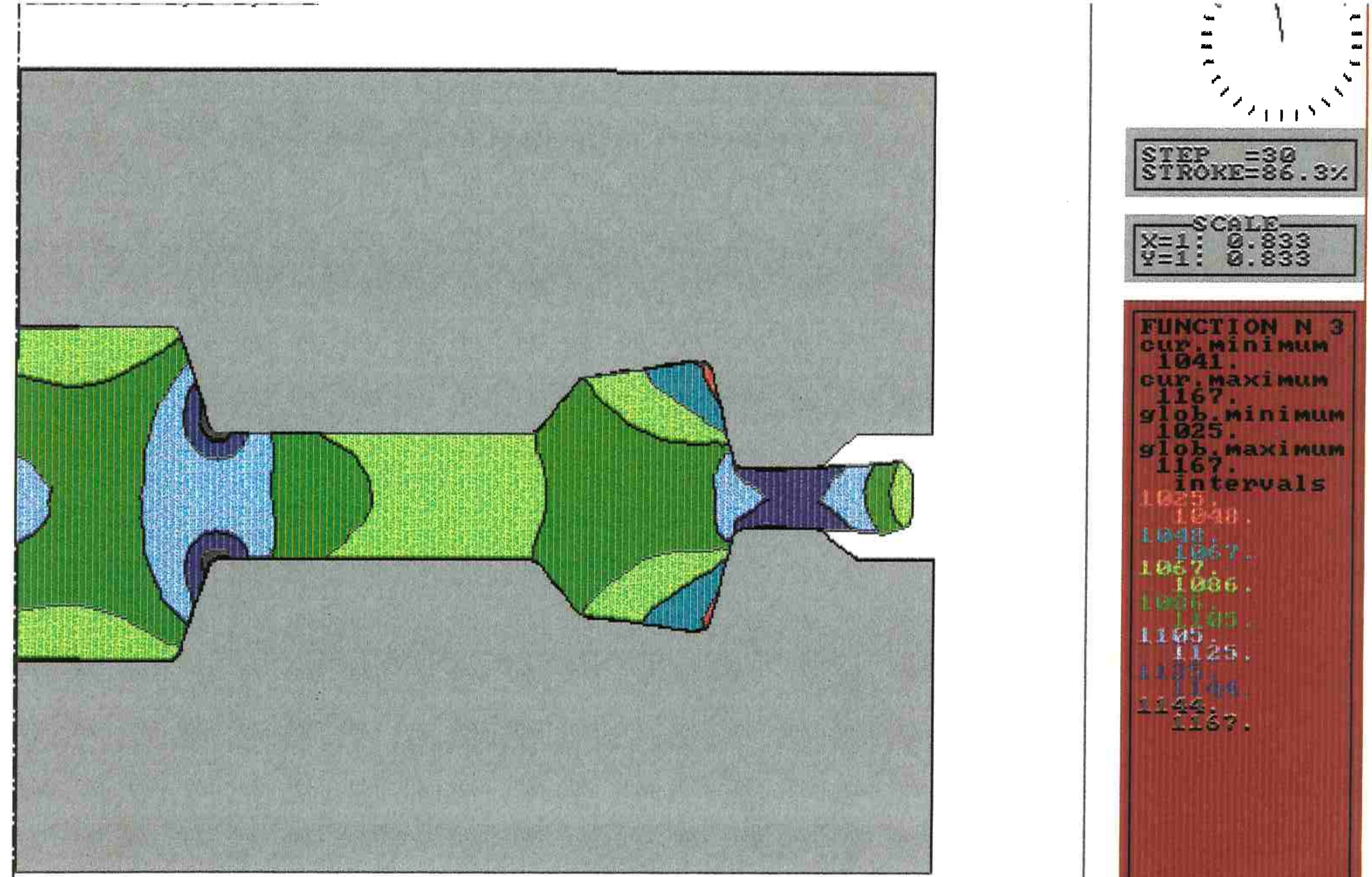

FIG. 3 DISTRIBUIÇÃO DA TEMPERATURA FORM-2D

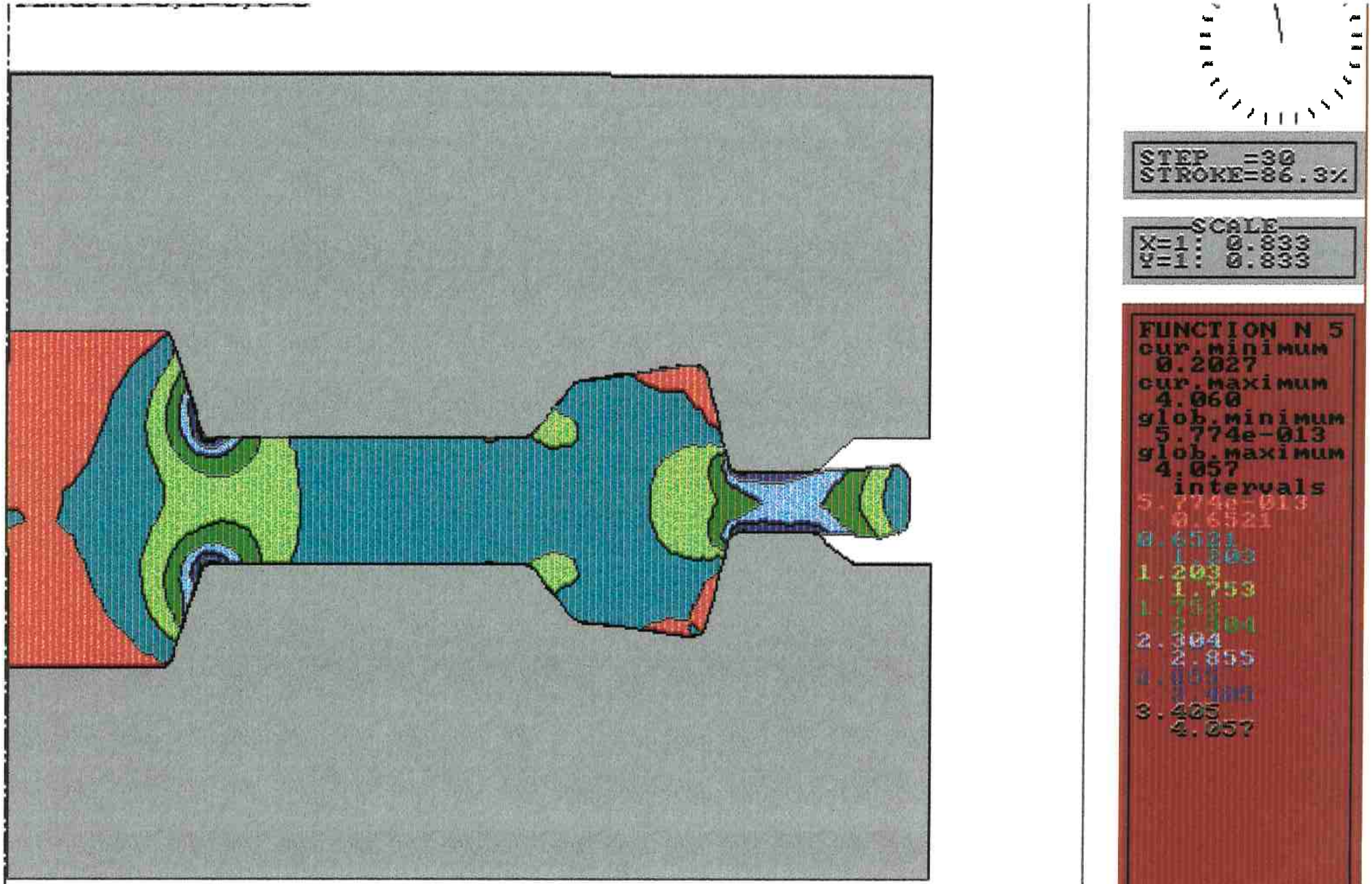

FIG.5 DISTRIBUIÇÃO DA DEFORMAÇÃO
FORM-2D

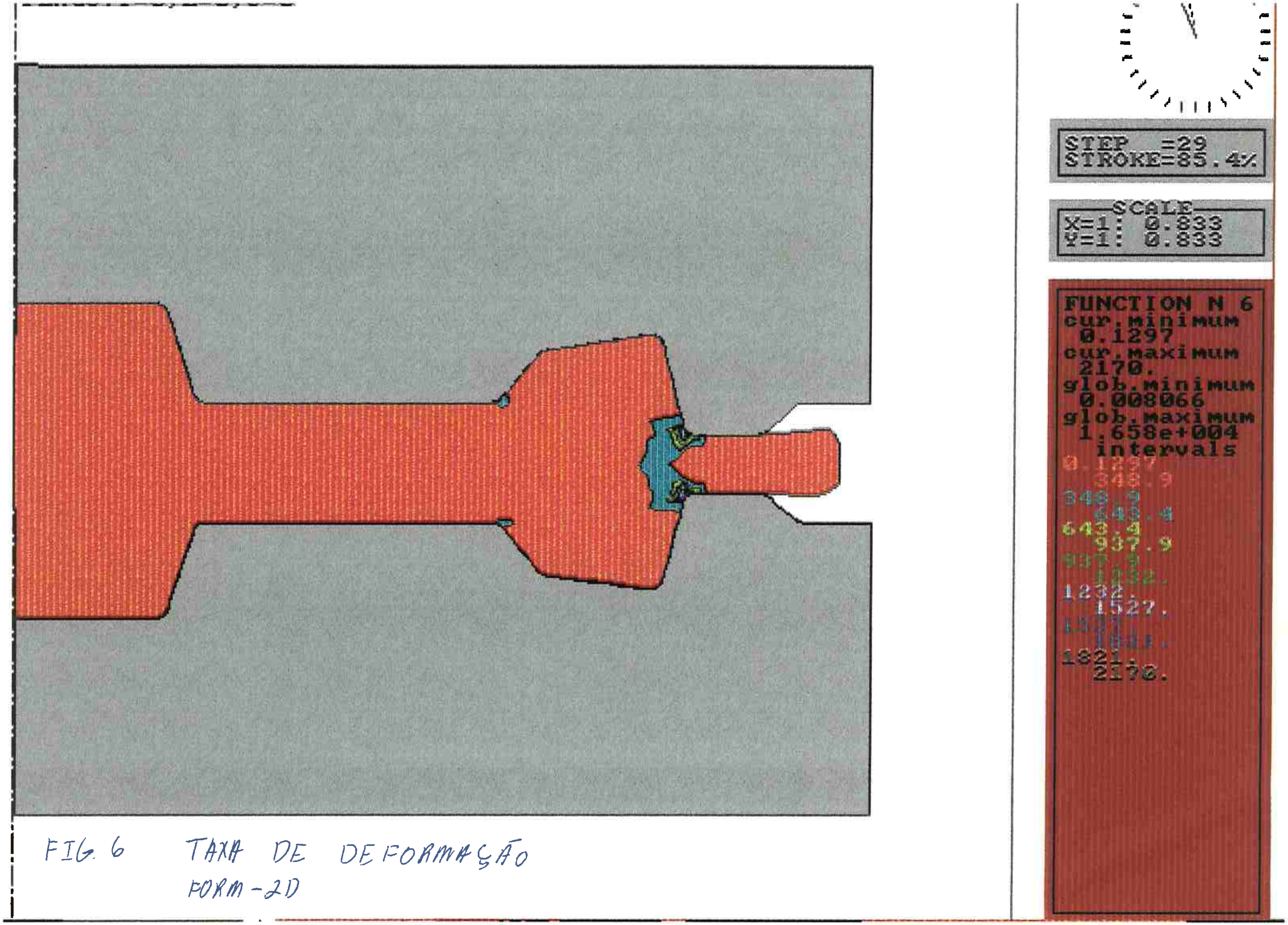

FIG. 6 TAXA DE DEFORMAÇÃO
FORM-2D

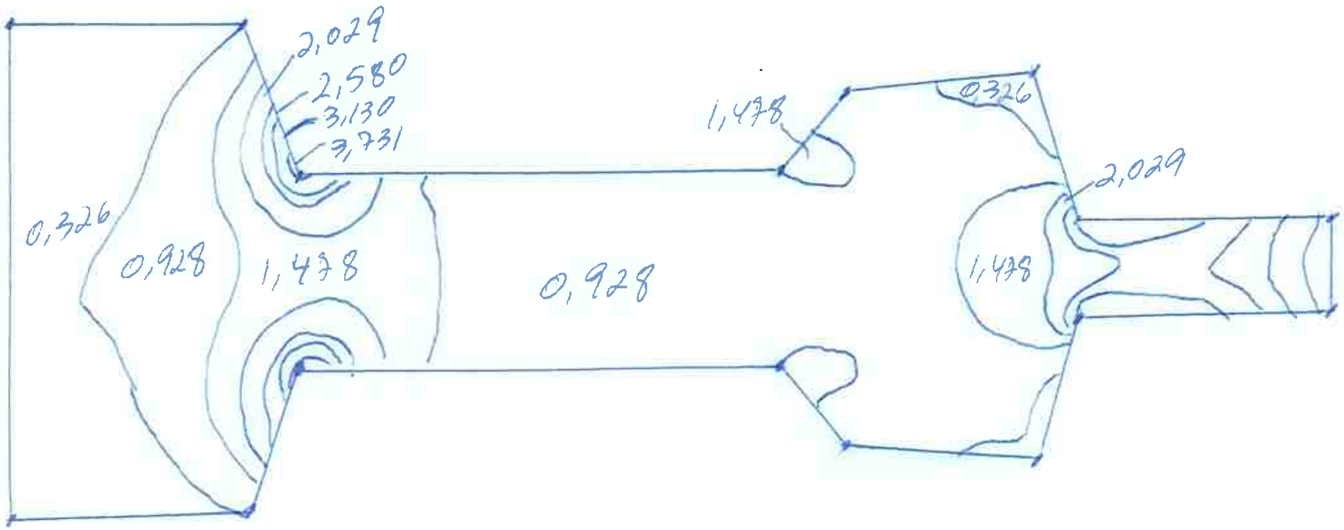

VALOR MÉDIO DA DEFORMAÇÃO

FIG 8

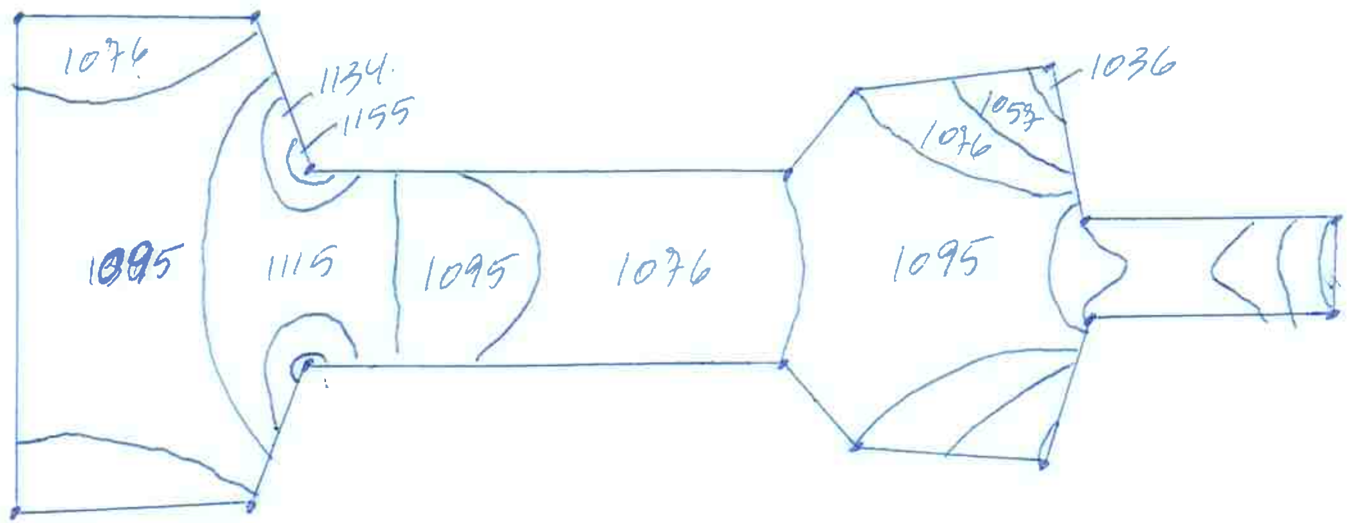

VALOR MÉDIO DA TEMPERTURA
FIG 9

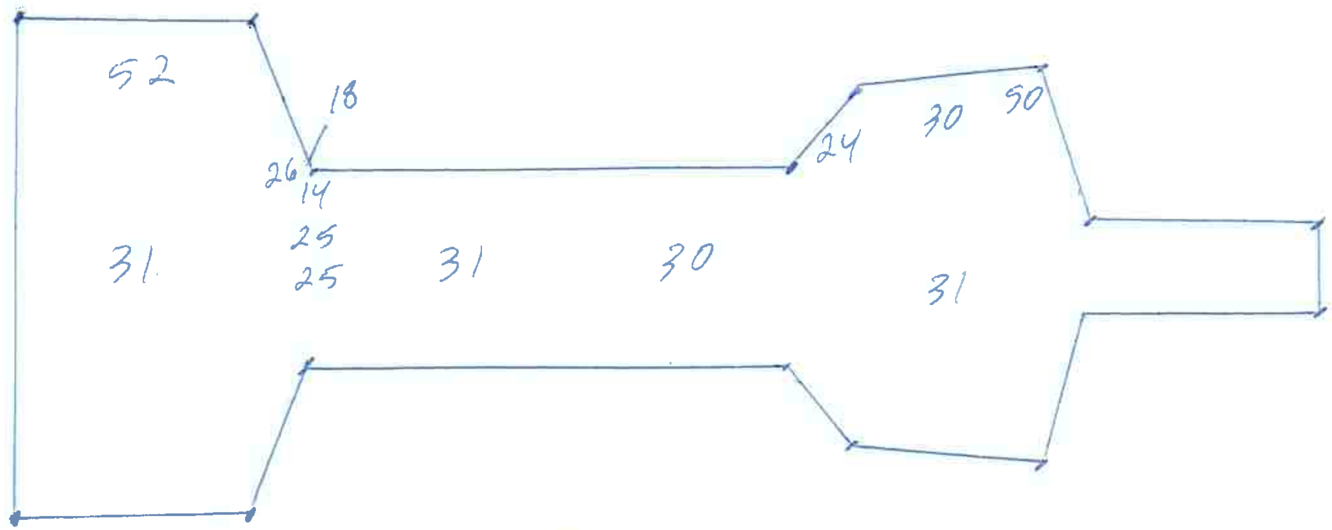

DISTRIBUIÇÃO DO TAMANHO DE GRÃO
FIG 7